RESOURCE ANNOUNCEMENT

Fungal Metabarcoding Data for Two Grapevine Varieties (Regent and *Vitis vinifera* 'Cabernet-Sauvignon') Inoculated with Powdery Mildew (*Erysiphe necator*) Under Drought Conditions

Corinne Vacher,[1,†] Claire Francioni,[2] Marion Michel,[2] Tania Fort,[1,3] Julie Faivre d'Arcier,[1] Emilie Chancerel,[1] François Delmotte,[2] and Chloé E. L. Delmas[2]

[1] INRAE, University of Bordeaux, BIOGECO, 33615, Pessac, France
[2] INRAE, Bordeaux Sciences Agro, ISVV, SAVE, 33140, Villenave d'Ornon, France
[3] Laboratory of Environmental Microbiology, Institute of Microbiology of the CAS, Vídeňská 1083, 14220 Praha 4, Czech Republic

Funding
This work was supported by the Agence Nationale de la Recherche (French National Research Agency [ANR]) through LabEx COTE (ANR-10-LABX-45) within the "VIVALDI" project and under grants ANR-17-CE32-0011 (ANR NGB) and 20-PCPA-0010 (PPR VITAE). Additional funding was received from the Conseil Régional Aquitaine (Aquitaine Region) (Athene project number 2016-1R20301-00007218).

Keywords
disease, drought stress, *Erysiphe necator*, fungal communities, grapevine, metabarcoding, plant microbiome, powdery mildew, *Vitis vinifera*

Resource Announcement

Plants live in association with diversified communities of microorganisms that promote their growth and contribute to their resistance to microbial pathogens and insect pests and to their tolerance to abiotic stressors, including drought (Hacquard et al. 2017; Hardoim et al. 2015; McLaren and Callahan 2020; Ngumbi and Kloepper 2016; Pineda et al. 2017). The increasing needs of humanity for food supply, the need to reduce fertilizer and pesticide use to protect human and environmental health, and the threats of climate change and disease emergence all provide incentives to use microorganisms to promote crop growth and health (Busby et al. 2017; D'Hondt et al. 2021; Toju et al. 2018). One of the challenges currently facing us is discovering and identifying microbial strains or consortia capable of alleviating biotic and abiotic stresses, and integrating them into crop management (Berg et al. 2017; Poudel et al. 2016).

Addressing this challenge is crucial in the case of European cultivated grapevine (*Vitis vinifera* L.) because this emblematic crop is a very heavy user of phytosanitary products (mainly copper, sulfur and synthetic chemical fungicides targeting leaf diseases). Strengthening microbial biocontrol of grapevine leaf diseases by stimulating the microbiota naturally present in vineyards or by inoculating new microorganisms (Bartoli et al. 2020) could reduce viticulture reliance on chemical fungicides. However, this nature-based solution (Maes and Jacobs 2017) will only be effective and sustainable if microbial antagonisms are resilient to microclimatic and climatic variations and associated changes in vine physiology. This is why vine–pathogen–microbiota interactions should be studied under a range of abiotic conditions. Powdery mildew is one of the grapevine leaf diseases for which the use of chemical fungicides must be reduced. It is caused by the ascomycete fungus *Erysiphe necator* (Armijo et al. 2016;

†Corresponding author: C. Vacher; corinne.vacher@inrae.fr

Author contributions: C.E.L.D. and F.D. designed the study; C.E.L.D., C.F., and M.M. collected samples and metadata; T.F., J.F.A., and E.C. performed the molecular biology work; C.V. performed data analysis and wrote the manuscript; and all of the authors edited the manuscript.

e-Xtra: Supplementary material is available online.

The author(s) declare no conflict of interest.

Accepted for publication 6 July 2022.

Copyright © 2022 The Author(s). This is an open access article distributed under the CC BY-NC-ND 4.0 International license.

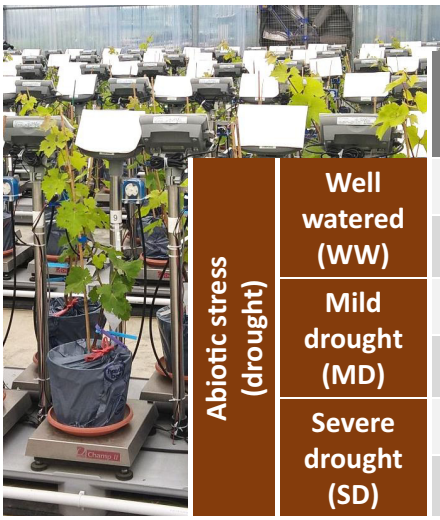

Abiotic stress (drought)	Plant variety	Control (no biotic stress)	Biotic stress (pathogen inoculation) 3 dpi	6 dpi	9 dpi	13 dpi	17 dpi	21 dpi
Well watered (WW)	CS	×3	×3	×3	×3	×3	×3	×3
	RE	×3	×3	×3	×3	×3	×3	×3
Mild drought (MD)	CS	×3	×3	×3	×3	×3	×3	×3
	RE	×3	×3	×3	×3	×3	×3	×3
Severe drought (SD)	CS	×3	×3	×3	×3	×3	×4	×3
	RE	×3	×3	×3	×3	×3	×3	×3

Fig. 1. Sampling design. Two grapevine varieties (Cabernet-Sauvignon [CS] and Regent [RE]) were subjected to a combination of biotic stress (pathogen inoculation) and abiotic stress (drought) in a controlled experiment. Plants were placed on an automated minilysimeter greenhouse platform with continuous weighing of the pots (picture on the left). The water stress was induced by stopping irrigation on two different dates and was monitored using leaf water potential (see text for details). The leaf microbiota was characterized for 108 inoculated samples, corresponding to 2 grapevine varieties (RE or CS) × 3 drought treatments (well-watered [WW], moderate drought [MD], or severe drought [SD]) × 3 individuals × 6 sampling dates (3, 6, 9, 13, 17, and 21 days postinoculation [dpi]). We also collected 18 control leaf samples, corresponding to 2 grapevine varieties (RE or CS) × 3 drought treatments (WW, MD, or SD) × 3 individuals, on a single date (corresponding to 6 dpi). These control samples were not inoculated with the pathogen. An additional inoculated leaf sample was collected for the CS variety in the SD treatment at 17 dpi, increasing to 127 the total number of leaf samples.

Gadoury et al. 2012), an obligate biotrophic pathogen that infects living cells in grapevine green tissues and then diverts nutrients from the cells without killing them. Although this fungus triggers significant yield losses worldwide, little is known about its interactions with the grapevine microbiota (Panstruga and Kuhn 2019). Even less is known about the response of these pathogen–microbiota interactions to the abiotic environment, including drought events that will increase in frequency and intensity in the coming decades (Spinoni et al. 2018). The data provided could contribute to filling this knowledge gap.

Here, we provide fungal metabarcoding data associated with powdery mildew leaf lesions (caused by inoculation with the pathogen *E. necator*) as a function of time from inoculation, for two grapevine varieties (the partially disease-resistant variety Regent and the susceptible *V. vinifera* 'Cabernet-Sauvignon') subjected to three levels of drought stress. In addition to this temporal dataset, we provide a smaller baseline dataset describing fungal communities in control, noninoculated leaf samples. For both datasets, we provide the raw fungal metabarcoding data, the amplicon sequence variant (ASV) tables obtained after bioinformatic processing, the metadata describing experimental conditions, and the code used for bioinformatic analysis and descriptive statistical analysis. We performed only simple and descriptive statistical analyses to highlight the structure of the metabarcoding datasets. We anticipate that more advanced statistical analyses, in combination with other grapevine microbiome datasets, might contribute to (i) decipher the interactions between *E. necator* and other microorganisms, (ii) assess the relative influence of the grapevine leaf microbiota on the development of powdery mildew compared with that of plant genetic resistance and drought stress, (iii) help define the "core mycobiome" of European cultivated grapevine and, more generally, (iv) understand the responses of microbial communities to multiple environmental stressors.

Materials and Methods

Experimental design. *Plant material and growth conditions.* Samples were collected in a greenhouse experiment (Fig. 1) conducted in June 2016 at the INRAE research center at Villenave d'Ornon, France (44°47′24.0″N, 0°34′33.6″W). Plants of two grapevine varieties—*V. vinifera* 'Cabernet Sauvignon' (CS, $n = 72$) and the variety Regent (RE, $n = 72$)—were produced and grafted onto the SO4 rootstock at the Reben Sibbus vine nursery (Sasbach

am Kaiserstuhl, Germany) in 2015. Cabernet-Sauvignon is susceptible to powdery mildew, like most *V. vinifera* cultivars (Gadoury et al. 2012), while Regent is a partially resistant hybrid (Fischer et al. 2004). They were grown in individual 5-liter pots filled with 1 kg of gravel and 4.5 kg of "terre de Couhins" (20% clay, 18% silt, and 62% sand). Plants were placed on an automated minilysimeter greenhouse platform with continuous weighing of the pots on individual scales to measure soil water availability and whole-plant transpiration in real time (Charrier et al. 2018; Dayer et al. 2020). Plants were grown under a natural photoperiod with average air humidity and temperature of 67.8% and 21.5°C, respectively. Each plant had two shoots, each carrying approximately eight leaves, at the start of the dry-down experiment.

Watering treatments. All plants were watered to saturation at the end of the afternoon and drained overnight (i.e. watered to field capacity) the day before the start of the dry-down experiment (10 May). Each plant was then randomly assigned to one of three different watering treatments. One-third of the plants ($n = 24$ of each variety) were irrigated to field capacity ("well-watered" plants [WW]), as demonstrated by their predawn water potential (ΨPD), which remained close to 0 MPa throughout the experiment. These plants received exactly the amount of water they consumed each day. The other plants were subjected to one of two levels of drought induced by stopping irrigation on two different dates, 1 week apart. Irrigation was stopped on 11 May to establish a "severe" drought stress (SD) for the second third of the plants ($n = 24$ of each variety). This SD was characterized by a mean $\Psi\text{PD} = -0.4$ MPa for both varieties at the time of inoculation with the pathogen (1 June) and a final ΨPD ranging from -1.61 to -2.05 MPa in RE and CS, respectively. The irrigation of the last third of the plants was stopped 1 week later, on 17 May, to induce "mild" drought stress (MD) with a mean $\Psi\text{PD} = -0.10$ and -0.23 MPa at the time of the pathogen inoculation and a final ΨPD of -1.2 to -1.6 MPa in RE and CS, respectively.

Pathogen inoculation. For each drought treatment (WW, MD, and SD), each plant was randomly assigned to one of two levels of pathogen exposure. Half the plants were inoculated with *E. necator* on 1 June, 3 weeks after the start of the dry-down experiment. The plants were then at the 10-leaf stage. The strain used for inoculation was isolated from an infected Cabernet-Sauvignon leaf collected from a plant production greenhouse (INRAE, La Grande Ferrade). This strain was then propagated on Cabernet-Sauvignon leaves placed adaxial-side-up on agar (20 g liter^{-1}) containing benzimidazole (30 mg liter^{-1}) in Petri dishes, until enough inoculum was obtained, as described by Delye and Corio-Costet (1998). To obtain a homogeneous spore distribution on the leaves used as source of inoculum for the experiment, conidia were blown within a settling tower placed above the source inoculum leaves, as described by Cartolaro and Steva (1990) and Calonnec et al. (2018). Leaves of the experiment were inoculated by gently touching a source inoculum leaf with a cotton swab, then the leaf to be inoculated with the cotton swab. The same pressure was exerted on the swab for each inoculation to standardize the number of spores transferred (108 conidia per inoculation point, on average). We inoculated seven leaves per shoot, with six inoculations per leaf (Fig. 2A). The other half of the plants (hereafter referred to as control plants) were not inoculated and were treated with a chemical fungicide (tebuconazole, 0.02 g/liter, Corail; Bayer CropScience) on 23 May. The fungicide treatment prevented *E. necator* infections in the control plants (especially in the highly susceptible Cabernet-Sauvignon plants), because control and inoculated plants were randomly placed in the same greenhouse and in close proximity. If we had not applied the fungicide, the control Cabernet-Sauvignon plants would have been naturally infected with *E. necator* and we would not have been able to maintain two levels of pathogen exposure throughout the experiment. Tebuconazole is a 1,2,4-triazole fungicide, like penconazole, which is known to have little effect on grapevine foliar fungal communities (Perazzolli et al. 2014). Nevertheless, we cannot exclude the possibility that the fungicide application altered the microbiota of the control plants. Therefore, we did not sample the leaves of the control plants immediately after the fungicide treatment. We let 15 days pass so that the microbiota could reassemble after the disruption caused by the fungicide treatment (control leaves were collected on 6 June).

Leaf sampling. In total, 127 leaf samples were collected during the experiment (Fig. 1). Leaf disks were collected from leaves of the same age on three inoculated plants per variety and per drought treatment, on six dates (3, 6, 9, 13, 17, and 21 days postinoculation [dpi]). For each date, the 3 sampled plants were chosen randomly among the 12 inoculated plants representing the variety–drought treatment combination. One disk of 1 cm in diameter, centered

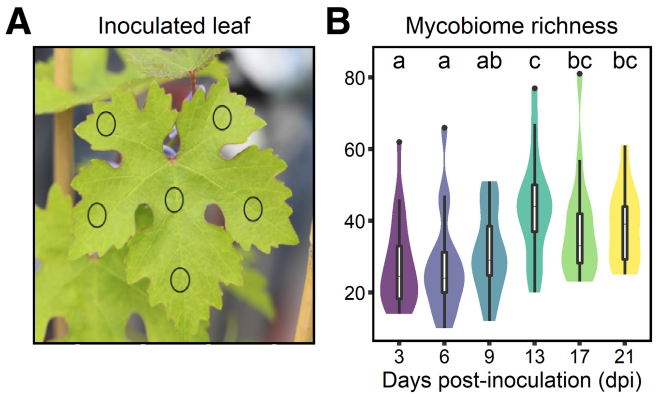

Fig. 2. Variation in foliar fungal community richness after inoculation with powdery mildew (*Erysiphe necator*). **A,** Photograph of a Cabernet-Sauvignon leaf just after inoculation. Black circles indicate the six inoculation points. **B,** Temporal variations in fungal community richness after inoculation with *E. necator*. Community richness was defined as the number of amplicon sequence variants (ASVs) per sample. The effect of time (measured in days postinoculation [dpi]) was significant (Supplementary Table S2A), according to a negative binomial generalized linear model followed by a type II analysis of variance. Letters indicate the results of pairwise Wilcoxon rank sum tests with a Benjamini-Hochberg correction for multiple testing. Richness was estimated for the residential fungal community (i.e. the fungal community without the inoculated pathogen species, *E. necator*). Data from the two vine varieties and the three drought treatments were pooled because these two factors had no effect on residential community richness (Supplementary Table S2A).

on an inoculation point (Fig. 2A), was collected from each chosen plant on each date with a sterilized hole-punch in the sterile environment of a MICROBIO electric burner (MSEI). The leaf disk was immediately placed in a 2-ml Eppendorf tube and stored in a dry shipper with liquid nitrogen. The samples were stored at −80°C in the laboratory until extraction. Disease stage, defined as sporulating lesion diameter, was assessed visually with a size standard (a pierced ruler) for each disk. Disease stage was scored from 0 to 4, where 0 = no lesion, 1 = sporulating lesion diameter from 0 to 7 mm, 2 = from 7 to 9 mm, 3 = from 9 to 10 mm, and 4 = lesion covering the whole disk and extending beyond it. Three samples had necrotic lesions without spore colonies (they were awarded a score of 7 in the metadata file). They were removed from the preliminary statistical analyses performed in the present study. Leaf disks were also collected from three control plants per variety and per drought treatment on the second sampling date (6 dpi) (Fig. 1). These 3 sampled plants were chosen randomly among the 12 control plants representing the variety–drought treatment combination.

Total DNA extraction. Leaf disks were ground frozen, at 1,500 rpm, with two 30-s pulses of a Geno/Grinder, with manual shaking between each grinding step. The plates were then centrifuged for 1 min at 6,200 rpm. Total genomic DNA was extracted with a plant DNA extraction kit, as in other studies (Behrens and Fisher 2022). We used the DNeasy Plant Mini Kit (Qiagen) according to the manufacturer's protocol, except that samples were subjected to two rounds of elution with 50 µl of elution buffer (10 mM Tris-HCl and 0.5 mM EDTA, pH 9.0) each.

Fungal internal transcribed spacer 1 amplification. The internal transcribed spacer 1 (ITS1) region of the fungal ITS ribosomal DNA gene (Schoch et al. 2012) was amplified with the ITS1F-ITS2 primers (Gardes and Bruns 1993; White et al. 1990). Each primer contained the Illumina adaptor sequence and a tag (ITS1F: 5′-CAAGCAGAAGACGGCATACGAGATGT GACTGGAGTTCAGACGTGTGCTCTTCCGATCTxxxxxxxxxxxxCTTGGTCATTTAGAGGAAG TAA-3′ and ITS2: 5′-AATGATACGGCGACCACCGAGATCTACACTCTTTCCCTACACGACGC TCTTCCGATCTxxxxxxxxxxxxGCTGCGTTCTTCATCGATGC-3′, where "x" is the 12-nucleotide tag), making it possible to overcome the need for a two-stage PCR. The PCR mixture (final volume = 20 µl) consisted of 10 µl of 2× QIAGEN Multiplex PCR Master Mix, 2 µl each of the forward and reverse primers (0.1 µM final concentration), 4 µl of water, 1 µl of bovine serum albumen (BSA) at 10 mg ml^{-1}, and 1 µl of DNA template. PCR was performed on a Veriti 96-well Thermal Cycler (Applied Biosystems) under the following conditions: initial denaturation at 95°C for 15 min; followed by 35 cycles of 94°C for 30 s, 57°C for 90 s, and 72°C for 90 s; and a final extension phase at 72°C for 10 min. The size and quality

of the amplification products was checked by electrophoresis in 2% agarose gels with 0.1% GelRed staining (Nucleic Acid Gel Stain, 10,000×; Biotium, Glowing Products for Science) and migration for 20 min at 100 V.

We performed amplifications for 6 molecular control samples in addition to the 127 leaf samples. Each of the two PCR plates carried one negative extraction control, one negative PCR control, and one positive PCR control. The negative extraction control consisted of a sample-free tube on the extraction plate, subjected to the same extraction and amplification procedures as the other samples. The negative PCR control consisted of a sample-free tube on the PCR plate, subjected to the same amplification procedure as all of the other samples. The positive controls for PCR consisted of tubes containing DNA from two marine fungal strains (*Candida oceani* and *Yamadazyma barbieri*) unlikely to be present in our samples. One of the positive PCR controls included 1 µl of DNA at 10 ng μl^{-1} from *C. oceani* and the other included 1 µl of DNA at 10 ng μl^{-1} from *Y. barbieri.*

Illumina MiSeq sequencing. PCR products were purified, quantified (Quant-it dsDNA assay kit; Invitrogen), and used to constitute equimolar pools (Hamilton Microlab STAR robot). Mean fragment size was determined with a Tapestation instrument (Agilent Technologies). Libraries were sequenced on one half run of the MiSeq Instrument (Illumina) with the reagent kit v2 (500 cycles). Sequence demultiplexing (with an exact index search) was performed at the PGTB sequencing facility (Genome Transcriptome Facility of Bordeaux, Pierroton, France) with DoubleTagDemultiplexer.

Bioinformatics. The dereplicated sequence files were deposited in the NCBI Sequence Read Archive (SRA) via the METAGENOTE platform (Quiñones et al. 2020), after the metadata file had been checked with the cloud-based tool Keemei (Rideout et al. 2016).

Bioinformatic analyses were performed in Docker v19.03.13 with QIIME2 v2020.8 (Bolyen et al. 2019) and the plugin q2-itsxpress v1.8.0 (Rivers et al. 2018). Fungal ITS1 regions were extracted from the dereplicated dataset with ITSxpress (Rivers et al. 2018). Denoising, assembly, and chimera removal were performed with DADA2 (Callahan et al. 2016), with default options for the *dada2 denoised-paired* function. Because ITS1 regions were extracted, we did not perform any truncation of the sequences at the 3′ and 5′ ends. Forward and reverse sequences with a number of expected errors > 2 were discarded. Remaining sequences were truncated at the first instance of a quality score ≤ 2. Forward and reverse sequences were assembled if there was at least a 12-nucleotide overlap between them. Samples were then denoised independently and chimeras were removed with the "consensus" method. Taxonomic assignments were performed with the latest "developer" version of the QIIME2-formatted UNITE database (version 04.02.2020) (Abarenkov et al. 2020) and the *feature-classifier* function (Bokulich et al. 2018).

We searched for putative contaminants by carefully examining the taxonomic composition of control samples and using the R decontam package v1.10.0 (Davis et al. 2018), after transformation of the data into an object interpretable by the R phyloseq package v1.34.0 (McMurdie and Holmes 2013) with the R package qiime2R v0.99.4 (Bisanz 2018) (Supplementary Methods S1). Two methods are available in the decontam package: the "frequency" method, which assumes that contaminants have a higher frequency in samples with a low DNA concentration before equimolar pooling, and the "prevalence" method, which assumes that contaminants have a higher prevalence in negative control samples than in environmental samples. In our dataset, the DNA concentration of the samples inoculated was significantly correlated with the number of days since inoculation (Spearman's $\rho = 0.564$, *P* value < 0.001) and disease stage ($\rho = 0.585$, *P* value < 0.001), suggesting that the frequency method might misclassify fungal ASVs associated with younger and healthier leaves as contaminants, fungal DNA amplification being more difficult in this context. In particular, it was thought that the frequency method might remove ASVs negatively associated with the pathogen *E. necator* (i.e. putative antagonists). Therefore, we used the prevalence method with a stringent threshold (=0.5) that classified all ASVs more prevalent in negative controls than in environmental samples as contaminants. We also removed putative cross-contaminants by filtering out the rarest ASVs within each sample. The frequency threshold below which an ASV was removed was defined as the highest frequency of a noncontrol ASV in a positive control sample. Finally, samples for which <1,000 sequences were obtained were removed.

Descriptive statistics. All statistical analyses were performed with R v4.2.0 (R Core Team 2021). We first investigated the effects of vine variety, drought treatment, and their

interaction on fungal community richness, diversity, and composition in control leaf samples. Community richness was defined as the total number of ASVs per sample. Community diversity for each sample (i.e. α-diversity) was assessed with the inverse Simpson diversity index. Compositional dissimilarities between samples (i.e. β-diversity) were assessed by calculating the Canberra or Pearson distance and visualized in principal coordinate analysis (PcoA) and nonmetric multidimensional scaling analysis (NMDS), respectively. The combinations of Canberra distance with PcoA and of Pearson distance with NMDS are the best options for detecting clusters and gradients in community composition, respectively (Kuczinski et al. 2010). These community properties were calculated on a rarefied dataset. Rarefaction mitigates sequencing depth artifacts more effectively than other normalization techniques, thereby improving the detection of biological effects, especially when sequencing depth values are low and heterogeneous between samples (Weiss et al. 2017). The random subsampling of sequences (without replacement) was performed with the rarefy_even_depth function of the R phyloseq package v1.40.0 (McMurdie and Holmes 2013). Generalized linear models (GLMs), followed by a type II analysis of variance (ANOVA), were used to analyze the effects of vine variety, drought treatment, and their interaction on community richness and diversity. A negative binomial GLM with a log link function was used to model richness counts, whereas a Gaussian GLM with an identity link function was used to model community diversity. Permutational ANOVA (PERMANOVA) was used to analyze the effects of vine variety, drought treatment, and their interaction on community composition.

Then, we analyzed the effects of vine variety, drought treatment, disease development, and their interactions on the richness, diversity, and composition of the residential fungal community (i.e. the fungal community without the pathogen *E. necator*) in inoculated leaf samples. All of the ASVs assigned to *E. necator* were removed before rarefaction and statistical analysis. In silico depletion of reads assigned to a pathogen species is commonly used to assess the effects of a fungal pathogen on a fungal community (Durán et al. 2021; Jakuschkin et al. 2016). The depletion ensures that changes in community richness, diversity, and composition are not due to the pathogen itself. The relative abundance of the pathogen (or another variable representing disease development) can then be used as an explanatory variable for changes in the fungal community. The statistical methods used were identical to those for control samples. Three variables were used to describe disease development: the number of days since inoculation, a visual assessment of disease symptoms (disease stage), and the percentage of reads assigned to *E. necator* in the metabarcoding dataset (pathogen frequency). The correlation between these three variables was assessed by calculating Spearman's correlation coefficient. The three samples with necrotic lesions without colonies were removed, so that disease stage represented sporulating lesion size.

Results

Sequence data, ASV tables, and metadata. This Resource Announcement provides the raw sequence data, together with the raw and filtered ASV tables in QIIME2 format (Bolyen et al. 2019) and R phyloseq format (McMurdie and Holmes 2013). Summary statistics for the raw and filtered ASV tables and interactive taxonomic plots (.qzv files) can be viewed in the QIIME2view interface (https://view.qiime2.org/). In addition, the Resource Announcement provides three rarefied ASV tables in R phyloseq format that were used in the present study to perform descriptive statistical analyses and could be analyzed in the future with more advanced techniques.

The raw ASV table ('table.qza' and 'Raw_dataset_ps.RData') consists of 4,436,907 sequences representing 1,909 fungal ASVs distributed in 133 samples (corresponding to 127 grapevine leaf samples and 6 molecular control samples). In brief, the dereplicated sequence dataset contained 5,552,444 sequences, with a mean of 41,748 sequences per sample. The number of sequences per leaf sample ranged from 26 to 96,961. After extraction of the fungal ITS1 region with ITSxpress (Rivers et al. 2018), the dataset contained 4,793,443 sequences. After denoising, assembly, and chimera removal with DADA2 (Callahan et al. 2016), the dataset contained 4,436,907 sequences, among which DADA2 identified 1,909 ASVs.

The filtered ASV table ('filtered_dataset_ps.RData') was obtained by removing putative contaminants and cross-contaminants, the six molecular control samples, and one leaf sample with $<$1,000 sequences. It consists of 4,364,858 sequences representing 1,856 fungal

ASVs distributed in 126 grapevine leaf samples. The number of sequences per leaf sample ranged from 1,216 to 86,249, with a mean of 34,642 sequences per sample.

The first rarefied ASV table ('ps_control_rar.RData') corresponds to the whole fungal community in control, noninoculated leaf samples (Fig. 1). The rarefaction threshold was set to 3,000 sequences per sample according to rarefaction curves (Supplementary Fig. S1A). The rarefied ASV table represents the distribution of 279 fungal ASVs in 17 grapevine leaf samples. This table was used in the present study to assess the effects of vine variety, drought treatment, and their interactions on fungal community richness, diversity, and composition in control samples.

The second rarefied ASV table ('ps_inoc_rar.RData') corresponds to the whole fungal community in inoculated leaf samples (Fig. 1). The rarefaction threshold was set to 10,000 sequences per sample according to rarefaction curves (Supplementary Fig. S1B). The rarefied ASV table represents the distribution of 1,628 fungal ASVs in 95 grapevine leaf samples. This table was not analyzed in the present study but it could be used in the future to decipher pathogen-microbiota interactions.

The third rarefied ASV table ('ps_no_patho_rar.RData') represents the residential fungal community (i.e. the fungal community without the inoculated pathogen species, *E. necator*) in the inoculated samples (Fig. 1). The rarefaction threshold was set to 3,000 sequences per sample according to rarefaction curves (Supplementary Fig. S1C). The rarefied ASV table represents the distribution of 1,510 fungal ASVs in 91 grapevine leaf samples. This table was used in the present study to assess the effects of vine variety, drought treatment, disease development, and their interactions on the residential fungal community richness, diversity and composition.

Finally, in addition to sequence data and ASV tables, this Resource Announcement provides the following list of metadata for each sample: sample type (leaf sample or molecular control), DNA concentration before equimolar pool, plant individual, plant variety (CS or RE), drought treatment (WW, MD, or SD), level of exposure to the pathogen (inoculated or control), sampling date, days since inoculation at the time of sampling (3, 6, 9, 13, 17, or 21 dpi), and disease stage (on a range from 0 to 4).

Factors structuring fungal communities in control versus inoculated leaves. Statistical analyses on control leaf samples ($n = 17$) revealed that vine variety influenced fungal community richness, in interaction with the drought treatment (Supplementary Table S1A), and had a marginally significant effect on fungal community diversity (Supplementary Table S1B), with a trend toward a higher diversity for the Regent variety (Supplementary Fig. S2).

Statistical analysis of inoculated leaf samples ($n = 91$) revealed that the richness of the residential fungal community varied significantly with days since inoculation and had a tendency to increase from 9 dpi (Supplementary Table S2A; Fig. 2B), the time point at which the first symptoms of *E. necator* infection appeared. The residential fungal community composition also changed significantly with days since inoculation (Supplementary Table S2C) but the effect was small, with days since inoculation accounting for only 1.2% of the variation in community composition. Similar results were obtained with disease stage or pathogen frequency instead of days since inoculation, because all three variables were correlated (Supplementary Fig. S3). These results are not shown here because the best GLM and PERMANOVA models were obtained with days since inoculation, according to the Akaike Information Criterion (AIC) and the percentage of variance explained, respectively (Supplementary Table S3).

Future Directions

This Resource Announcement provides a metabarcoding dataset describing the temporal dynamics of the leaf mycobiome for two grapevine varieties (the partially disease-resistant variety Regent and the susceptible *V. vinifera* 'Cabernet-Sauvignon') grown in a greenhouse under controlled biotic and abiotic (i.e., disease and drought) stress conditions. Simple statistical analysis of this metabarcoding dataset revealed that the mycobiome is structured by disease development in leaves inoculated with the foliar fungal pathogen *E. necator*, whereas it is shaped by grapevine variety in control, noninoculated leaves.

We believe that more advanced statistical analysis of this dataset could contribute to the development of a general framework of knowledge about the ways in which microbial communities respond to multiple environmental stressors. For instance, the dataset can be included in meta-analyses, such as those of the Microbiome Stress Project (Rocca et al. 2019).

Moreover, it can be combined with other grapevine mycobiome datasets (Barroso-Bergadà et al. 2021; Fort et al. 2016; Liu and Howell 2021; Varanda et al. 2016) to define the grapevine core mycobiome, a prerequisite for the development of sustainable viticulture (Toju et al. 2018).

We also expect this dataset to be useful for understanding the role of the leaf microbiome in the development of grapevine powdery mildew. First, this data may improve our understanding of the pathobiome of *E. necator* under various drought conditions. Based on differential abundance analysis methods (Weiss et al. 2017) and advanced methods of microbial network inference (Barroso-Bergadà et al. 2022; Röttjers and Faust 2018; Tackmann et al. 2019), this dataset may allow us to generate hypotheses of interactions between *E. necator* and other leaf microorganisms. Together with other grapevine microbiome datasets, it may facilitate the discovery of putative antagonists of powdery mildew, which could be integrated into disease biocontrol strategies after experimental testing. The strength of this dataset lies in the combination of controlled watering treatments and controlled fungal inoculation, providing insight into the robustness of antagonistic relationships in a context of climate change. Second, the dataset can be used to assess the relative influence of plant genetic resistance, drought conditions, and leaf microbiome diversity and composition on the development of grapevine powdery mildew. Finally, the combination of this dataset with the physiological and hormonal measurements performed at the individual plant level in the experiment will shed light on the roles of plant immunity and plant microbiota in the joint control of plant pathogen development (Hacquard et al. 2017) for grapevine powdery mildew.

Availability of Data and Materials

The sequence dataset has been deposited in NCBI SRA in bioproject PRJNA678415 (accession numbers SRX9508880 to SRX9508748) (https://www.ncbi.nlm.nih.gov/bioproject/678415). Bioinformatic scripts and raw and filtered ASV tables in QIIME2 format and R phyloseq format have been deposited in Dataverse (https://doi.org/10.15454/KMAU1G). The statistical analysis scripts and rarefied ASV tables used for the analyses have been deposited in Dataverse (https://doi.org/10.15454/PL3HWQ).

Acknowledgments

We thank all members of the PGTB sequencing facility (Genome Transcriptome Facility of Bordeaux, Pierroton, France) for their support in molecular biology; G. Burgaud for kindly providing the marine fungal strains used as positive controls; UMR EGFV for providing access to the minilysimeter platform (Bord'ô) and support for its use; UMR SAVE for providing technical help with experimentation; J. Vallance and C. Pauvert for helpful discussions at the beginning of the experiment; J. Sappa from Alex Edelman & Associates for English language revision of the first version of the manuscript; and three anonymous reviewers for their careful reading of the manuscript and relevant comments.

Literature Cited

Abarenkov, K., Zirk, A., Piirmann, T., Pöhönen, R., Ivanov, F., Nilsson, R. H., and Kõljalg, U. 2020. UNITE QIIME release for Fungi. UNITE Community.

Armijo, G., Schlechter, R., Agurto, M., Muñoz, D., Nuñez, C., and Arce-Johnson, P. 2016. Grapevine pathogenic microorganisms: Understanding infection strategies and host response scenarios. Front. Plant Sci. 7:382.

Barroso-Bergadà, D., Pauvert, C., Vallance, J., Delière, L., Bohan, D. A., Buée, M., and Vacher, C. 2021. Microbial networks inferred from environmental DNA data for biomonitoring ecosystem change: Strengths and pitfalls. Mol. Ecol. Resour. 21: 762-780.

Barroso-Bergadà, D., Tamaddoni-Nezhad, A., Muggleton, S. H., Vacher, C., Galic, N., and Bohan, D. A. 2022. Machine learning of microbial interactions using abductive ILP and hypothesis frequency/compression estimation. Pages 26-40 in Int. Conf. Inductive Logic Programming. Springer, Cham, Switzerland.

Bartoli, C., Aubertot, J.-N., Litrico-Chiarelli, I., and Mougel, C. 2020. Protection agroécologique pour le maintien de la santé des plantes. Page 376 in: Biocontrôle. Éléments pour une protection agroécologique des cultures. X. Fauvergue, A. Rusch, M. Barret, M. Bardin, E. Jacquin-Joly, T. Malausa, and C. Lannou, eds. Editions Quae, Savoir Faire, Versailles, France.

Behrens, F. H., and Fischer, M. 2022. Evaluation of different phyllosphere sample types for parallel metabarcoding of Fungi and Oomycetes in *Vitis vinifera*. Phytobiomes J. 6:207-213.

Berg, G., Köberl, M., Rybakova, D., Müller, H., Grosch, R., and Smalla, K. 2017. Plant microbial diversity is suggested as the key to future biocontrol and health trends. FEMS Microbiol. Ecol. 93:fix050.

Bisanz, J. E. 2018. qiime2R: Importing QIIME2 artifacts and associated data into R sessions. https://github.com/jbisanz/qiime2R

Bokulich, N. A., Kaehler, B. D., Rideout, J. R., Dillon, M., Bolyen, E., Knight, R., Huttley, G. A., and Caporaso, J. G. 2018. Optimizing taxonomic classification of marker-gene amplicon sequences with QIIME 2's q2-feature-classifier plugin. Microbiome 6:90.

Bolyen, E., Rideout, J. R., Dillon, M. R., Bokulich, N. A., Abnet, C. C., Al-Ghalith, G. A., Alexander, H., Alm, E. J., Arumugam, M., Asnicar, F., Bai, Y., Bisanz, J. E., Bittinger, K., Brejnrod, A., Brislawn, C. J., Brown, C. T., Callahan, B. J., Caraballo-Rodríguez, A. M., Chase, J., Cope, E. K., Da Silva, R., Diener, C., Dorrestein, P. C., Douglas, G. M., Durall, D. M., Duvallet, C., Edwardson, C. F., Ernst, M., Estaki, M., Fouquier, J., Gauglitz, J. M., Gibbons, S. M., Gibson, D. L., Gonzalez, A., Gorlick, K., Guo, J., Hillmann, B., Holmes, S., Holste, H., Huttenhower, C., Huttley, G. A., Janssen, S.,

Jarmusch, A. K., Jiang, L., Kaehler, B. D., Kang, K. B., Keefe, C. R., Keim, P., Kelley, S. T., Knights, D., Koester, I., Kosciolek, T., Kreps, J., Langille, M. G. I., Lee, J., Ley, R., Liu, Y. X., Loftfield, E., Lozupone, C., Maher, M., Marotz, C., Martin, B. D., McDonald, D., McIver, L. J., Melnik, A. V., Metcalf, J. L., Morgan, S. C., Morton, J. T., Naimey, A. T., Navas-Molina, J. A., Nothias, L. F., Orchanian, S. B., Pearson, T., Peoples, S. L., Petras, D., Preuss, M. L., Pruesse, E., Rasmussen, L. B., Rivers, A., Robeson, M. S. 2nd, Rosenthal, P., Segata, N., Shaffer, M., Shiffer, A., Sinha, R., Song, S. J., Spear, J. R., Swafford, A. D., Thompson, L. R., Torres, P. J., Trinh, P., Tripathi, A., Turnbaugh, P. J., Ul-Hasan, S., van der Hooft, J. J. J., Vargas, F., Vázquez-Baeza, Y., Vogtmann, E., von Hippel, M., Walters, W., Wan, Y., Wang, M., Warren, J., Weber, K. C., Williamson, C. H. D., Willis, A. D., Xu, Z. Z., Zaneveld, J. R., Zhang, Y., Zhu, Q., Knight, R., and Caporaso, J. G. 2019. Reproducible, interactive, scalable and extensible microbiome data science using QIIME 2. Nat. Biotechnol. 37:852-857.

Busby, P. E., Soman, C., Wagner, M. R., Friesen, M. L., Kremer, J., Bennett, A., Morsy, M., Eisen, J. A., Leach, J. E., and Dangl, J. L. 2017. Research priorities for harnessing plant microbiomes in sustainable agriculture. PLoS Biol. 15:e2001793.

Callahan, B. J., McMurdie, P. J., Rosen, M. J., Han, A. W., Johnson, A. J. A., and Holmes, S. P. 2016. DADA2: High-resolution sample inference from Illumina amplicon data. Nat. Methods 13:581-583.

Calonnec, A., Jolivet, J., Vivin, P., and Schnee, S. 2018. Pathogenicity traits correlate with the susceptible *Vitis vinifera* leaf physiology transition in the biotroph fungus *Erysiphe necator*: An adaptation to plant ontogenic resistance. Front. Plant Sci. 9:1808.

Cartolaro, P., and Steva, H. 1990. Maîtrise de l'oïdium en laboratoire. Phytoma 419: 37-40.

Charrier, G., Delzon, S., Domec, J. C., Zhang, L., Delmas, C. E., Merlin, I., Corso, D., King, A., Ojeda, H., Ollat, N., Prieto, J. A., Scholach, T., Skinner, P., van Leeuwen, C., and Gambetta, G. A. 2018. Drought will not leave your glass empty: Low risk of hydraulic failure revealed by long-term drought observations in world's top wine regions. Sci. Adv. 4:eaao6969.

Davis, N. M., Proctor, D. M., Holmes, S. P., Relman, D. A., and Callahan, B. J. 2018. Simple statistical identification and removal of contaminant sequences in marker-gene and metagenomics data. Microbiome 6:226.

Dayer, S., Herrera, J. C., Dai, Z., Burlett, R., Lamarque, L. J., Delzon, S., Bortolami, G., Cochard, H., and Gambetta, G. A. 2020. The sequence and thresholds of leaf hydraulic traits underlying grapevine varietal differences in drought tolerance. J. Exp. Bot. 71:4333-4344.

Delye, C., and Corio-Costet, M. F. 1998. Origin of primary infections of grape by *Uncinula necator*: RAPD analysis discriminates two biotypes. Mycol. Res. 102:283-288.

D'Hondt, K., Kostic, T., McDowell, R., Eudes, F., Singh, B. K., Sarkar, S., Markakis, M., Schelkle, B., Maguin, E., and Sessitsch, A. 2021. Microbiome innovations for a sustainable future. Nat. Microbiol. 6:138-142.

Durán, P., Reinstädler, A., Rajakrut, A. L., Hashimoto, M., Garrido-Oter, R., Schulze-Lefert, P., and Panstruga, R. 2021. A fungal powdery mildew pathogen induces extensive local and marginal systemic changes in the *Arabidopsis thaliana* microbiota. Environ. Microbiol. 23:6292-6308.

Fischer, B. M., Salakhutdinov, I., Akkurt, M., Eibach, R., Edwards, K. J., Töpfer, R., and Zyprian, E. M. 2004. Quantitative trait locus analysis of fungal disease resistance factors on a molecular map of grapevine. Theor. Appl. Genet. 108:501-515.

Fort, T., Robin, C., Capdevielle, X., Delière, L., and Vacher, C. 2016. Foliar fungal communities strongly differ between habitat patches in a landscape mosaic. PeerJ 4:e2656.

Gadoury, D. M., Cadle-Davidson, L., Wilcox, W. F., Dry, I. B., Seem, R. C., and Milgroom, M. G. 2012. Grapevine powdery mildew (*Erysiphe necator*): A fascinating system for the study of the biology, ecology and epidemiology of an obligate biotroph. Mol. Plant Pathol. 13:1-16.

Gardes, M., and Bruns, T. D. 1993. ITS primers with enhanced specificity for basidiomycetes—Application to the identification of mycorrhizae and rusts. Mol. Ecol. 2:113-118.

Hacquard, S., Spaepen, S., Garrido-Oter, R., and Schulze-Lefert, P. 2017. Interplay between innate immunity and the plant microbiota. Annu. Rev. Phytopathol. 55: 565-589.

Hardoim, P. R., Van Overbeek, L. S., Berg, G., Pirttilä, A. M., Compant, S., Campisano, A., Döring, M., and Sessitsch, A. 2015. The hidden world within plants: Ecological and evolutionary considerations for defining functioning of microbial endophytes. Microbiol. Mol. Biol. Rev. 79:293-320.

Jakuschkin, B., Fievet, V., Schwaller, L., Fort, T., Robin, C., and Vacher, C. 2016. Deciphering the pathobiome: Intra-and interkingdom interactions involving the pathogen *Erysiphe alphitoides*. Microb. Ecol. 72:870-880.

Kuczynski, J., Liu, Z., Lozupone, C., McDonald, D., Fierer, N., and Knight, R. 2010. Microbial community resemblance methods differ in their ability to detect biologically relevant patterns. Nat. Methods 7:813-819.

Liu, D., and Howell, K. 2021. Community succession of the grapevine fungal microbiome in the annual growth cycle. Environ. Microbiol. 23:1842-1857.

Maes, J., and Jacobs, S. 2017. Nature-based solutions for Europe's sustainable development. Conserv. Lett. 10:121-124.

McLaren, M. R., and Callahan, B. J. 2020. Pathogen resistance may be the principal evolutionary advantage provided by the microbiome. Philos. Trans. R Soc. Lond. B Biol. Sci. 375:20190592.

McMurdie, P. J., and Holmes, S. 2013. phyloseq: An R package for reproducible interactive analysis and graphics of microbiome census data. PLoS One 8:e61217.

Ngumbi, E., and Kloepper, J. 2016. Bacterial-mediated drought tolerance: Current and future prospects. Appl. Soil Ecol. 105:109-125.

Panstruga, R., and Kuhn, H. 2019. Mutual interplay between phytopathogenic powdery mildew fungi and other microorganisms. Mol. Plant Pathol. 20:463-470.

Perazzolli, M., Antonielli, L., Storari, M., Puopolo, G., Pancher, M., Giovannini, O., Pindo, M., and Pertot, I. 2014. Resilience of the natural phyllosphere microbiota of the grapevine to chemical and biological pesticides. Appl. Environ. Microbiol. 80: 3585-3596.

Pineda, A., Kaplan, I., and Bezemer, T. M. 2017. Steering soil microbiomes to suppress aboveground insect pests. Trends Plant Sci. 22:770-778.

Poudel, R., Jumpponen, A., Schlatter, D. C., Paulitz, T. C., Gardener, B. M., Kinkel, L. L., and Garrett, K. A. 2016. Microbiome networks: A systems framework for identifying candidate microbial assemblages for disease management. Phytopathology 106:1083-1096.

Quiñones, M., Liou, D. T., Shyu, C., Kim, W., Vujkovic-Cvijin, I., Belkaid, Y., and Hurt, D. E. 2020. METAGENOTE: A simplified web platform for metadata annotation of genomic samples and streamlined submission to NCBI's sequence read archive. BMC Bioinf. 21:1-12.

R Core Team. 2021. R: A Language and Environment for Statistical Computing. R Foundation for Statistical Computing, Vienna, Austria. https://www.R-project.org/

Rideout, J. R., Chase, J. H., Bolyen, E., Ackermann, G., González, A., Knight, R., and Caporaso, J. G. 2016. Keemei: Cloud-based validation of tabular bioinformatics file formats in Google Sheets. GigaScience 5:s13742-016.

Rivers, A. R., Weber, K. C., Gardner, T. G., Liu, S., and Armstrong, S. D. 2018. ITSxpress: Software to rapidly trim internally transcribed spacer sequences with quality scores for marker gene analysis. F1000Res. 7:1418.

Rocca, J. D., Simonin, M., Blaszczak, J. R., Ernakovich, J. G., Gibbons, S. M., Midani, F. S., and Washburne, A. D. 2019. The microbiome stress project: Toward a global meta-analysis of environmental stressors and their effects on microbial communities. Front. Microbiol. 9:3272.

Röttjers, L., and Faust, K. 2018. From hairballs to hypotheses—Biological insights from microbial networks. FEMS Microbiol. Rev. 42:761-780.

Schoch, C. L., Seifert, K. A., Huhndorf, S., Robert, V., Spouge, J. L., Levesque, C. A., Chen, W., Bolchacova, E., Voigt, K., Crous, P. W., Miller, A. N., Wingfield, M. J., Aime, M. C., An, K.-D., Bai, F.-Y., Barreto, R. W., Begerow, D., Bergeron, M.-J., Blackwell, M., Boekhout, T., Bogale, M., Boonyuen, N., Burgaz, A. R., Buyck, B., Cai, L., Cai, Q., Cardinali, G., Chaverri, P., Coppins, B. J., Crespo, A., Cubas, P., Cummings, C., Damm, U., de Beer, Z. W., de Hoog, G. S., Del-Prado, R., Dentinger, B., Diéguez-Uribeondo, J., Divakar, P. K., Douglas, B., Dueñas, M., Duong, T. A., Eberhardt, U., Edwards, J. E., Elshahed, M. S., Fliegerova, K., Furtado, M., García, M. A., Ge, Z.-W., Griffith, G. W., Griffiths, K., Groenewald, J. Z., Groenewald, M., Grube, M., Gryzenhout, M., Guo, L.-D., Hagen, F., Hambleton, S., Hamelin, R. C., Hansen, K., Harrold, P., Heller, G., Herrera, C., Hirayama, K., Hirooka, Y., Ho, H.-M., Hoffmann, K., Hofstetter, V., Högnabba, F., Hollingsworth, P. M., Hong, S.-B., Hosaka, K., Houbraken, J., Hughes, K., Huhtinen, S., Hyde, K. D., James, T., Johnson, E. M., Johnson, J. E., Johnston, P. R., Jones, E. B. G., Kelly, L. J., Kirk, P. M., Knapp, D. G., Kõljalg, U., Kovács, G. M., Kurtzman, C. P., Landvik, S., Leavitt, S. D., Liggenstoffer, A. S., Liimatainen, K., Lombard, L., Luangsa-Ard, J. J., Lumbsch, H. T., Maganti, H., Maharachchikumbura, S. S. N., Martin, M. P., May, T. W., McTaggart, A. R., Methven, A. S., Meyer, W., Moncalvo, J.-M., Mongkolsamrit, S., Nagy, L. G., Nilsson, R. H., Niskanen, T., Nyilasi, I., Okada, G., Okane, I., Olariaga, I., Otte, J., Papp, T., Park, D., Petkovits, T., Pino-Bodas, R., Quaedvlieg, W., Raja, H. A., Redecker, D., Rintoul, T. L., Ruibal, C., Sarmiento-Ramírez, J. M., Schmitt, I., Schüßler, A., Shearer, C., Sotome, K., Stefani, F. O. P., Stenroos, S., Stielow, B., Stockinger, H., Suetrong, S., Suh, S.-O., Sung, Gi-Ho, Suzuki, M., Tanaka, K., Tedersoo, L., Telleria, M. T., Tretter, E., Untereiner, W. A., Urbina, H., Vágvölgyi, C., Vialle, A., Vu, T. D., Walther, G., Wang, Qi-M, Wang, Y., Weir, B. S., Weiß, M., White, M. M., Xu, J., Yahr, R., Yang, Z. L., Yurkov, A., Zamora, J.-C.,

Zhang, N., Zhuang, W.-Y., and Schindel, D. 2012. Nuclear ribosomal internal transcribed spacer (ITS) region as a universal DNA barcode marker for Fungi. Proc. Natl. Acad. Sci. U.S.A. 109:6241-6246.

Spinoni, J., Vogt, J. V., Naumann, G., Barbosa, P., and Dosio, A. 2018. Will drought events become more frequent and severe in Europe? Int. J. Climatol. 38:1718-1736.

Tackmann, J., Rodrigues, J. F. M., and von Mering, C. 2019. Rapid inference of direct interactions in large-scale ecological networks from heterogeneous microbial sequencing data. Cell Syst. 9:286-296.e8.

Toju, H., Peay, K. G., Yamamichi, M., Narisawa, K., Hiruma, K., Naito, K., Fukuda, S., Ushio, M., Nakaoka, S., Onoda, Y., Yoshida, K., Schlaeppi, K., Bai, Y., Sugiura, R., Ichihashi, Y., Minamisawa, K., and Kiers, E. T. 2018. Core microbiomes for sustainable agroecosystems. Nat. Plants 4:247-257.

Varanda, C. M. R., Oliveira, M., Materatski, P., Landum, M., Clara, M. I. E., and do Rosário Félix, M. 2016. Fungal endophytic communities associated to the phyllosphere of grapevine cultivars under different types of management. Fungal Biol. 120:1525-1536.

Weiss, S., Xu, Z. Z., Peddada, S., Amir, A., Bittinger, K., Gonzalez, A., Lozupone, C., Zaneveld, J. R., Vázquez-Baeza, Y., Birmingham, A., Hyde, E. R., and Knight, R. 2017. Normalization and microbial differential abundance strategies depend upon data characteristics. Microbiome 5:1-18.

White, T. J., Bruns, T., Lee, S., and Taylor, J. 1990. Amplification and direct sequencing of fungal ribosomal RNA genes for phylogenetics. Pages 315-322 in: PCR Protocols: A Guide to Methods and Applications. M. A. Innis, D. H. Gelfand, J. J. Sninsky, and T. J. White, eds. Academic Press, San Diego, CA, U.S.A.